

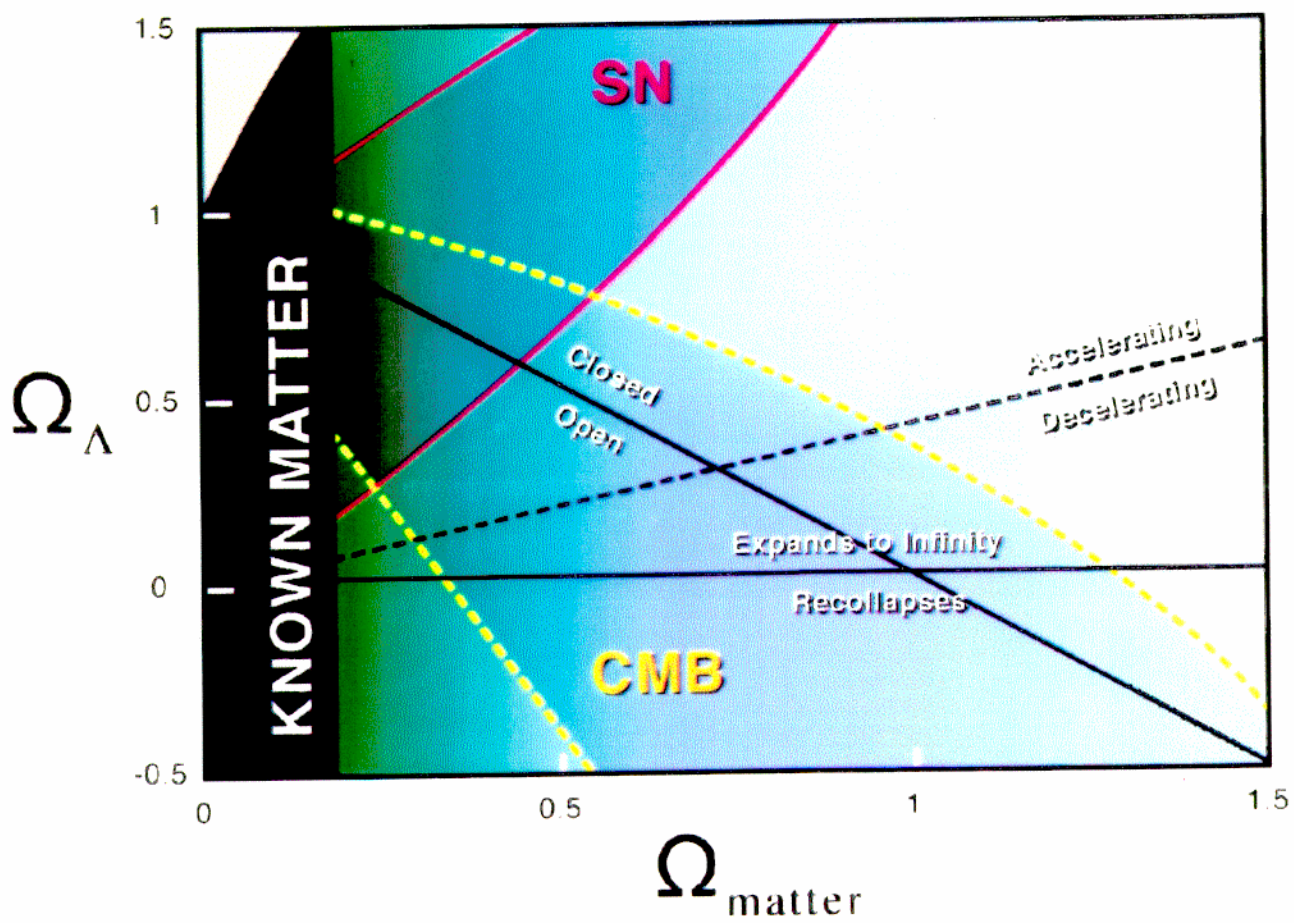
FUTURE DARK MATTER EXPLORATIONS VIA GRAVITATIONAL LENS TOMOGRAPHY

- Deep imaging in 2-degree fields; 500,000 arclets:

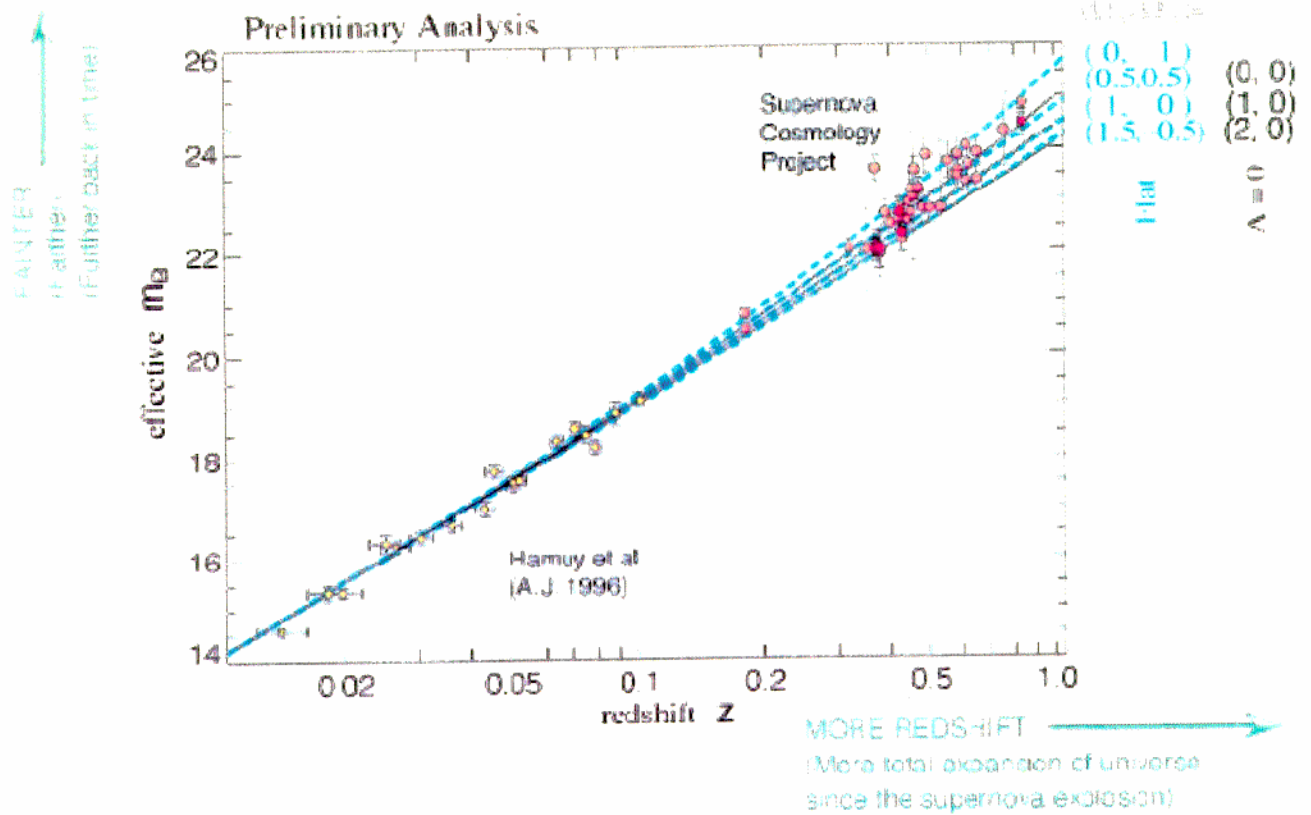
DARK MATTER TELESCOPE

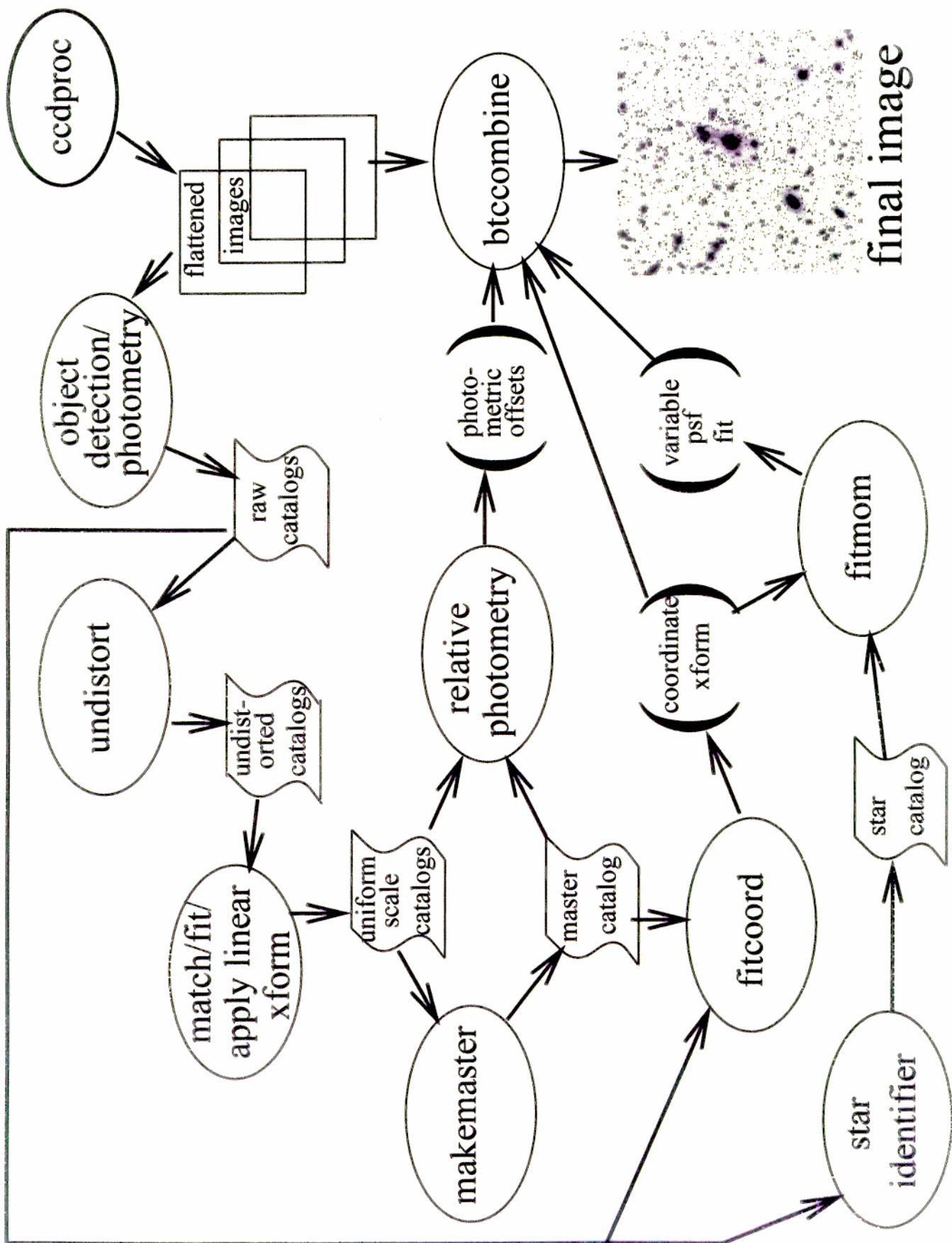
- Arclet spectroscopy: *KECK TELESCOPE*

- Structure of arclet source galaxies; Studies of strongly lensed cores of clusters: *HST*

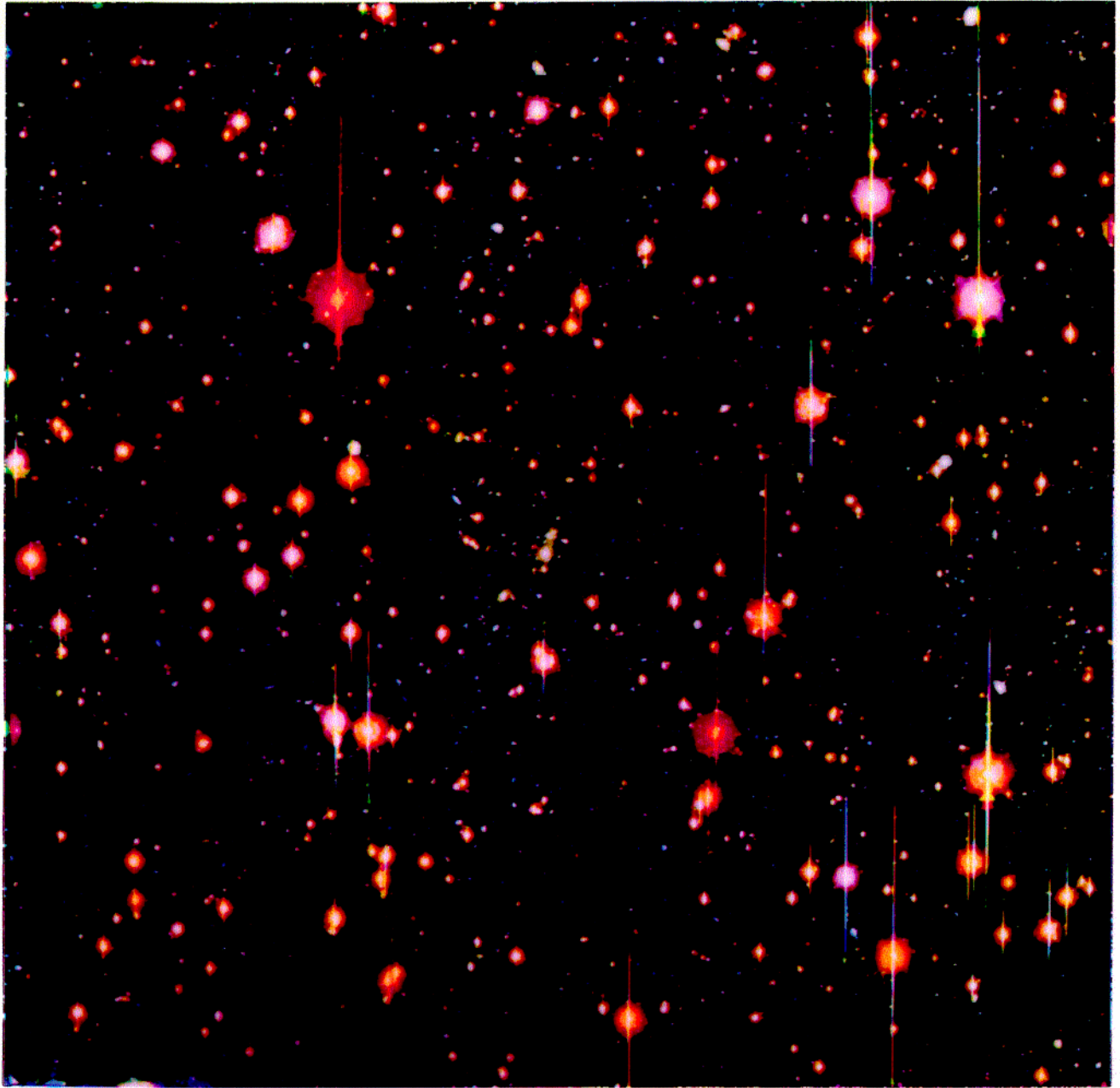


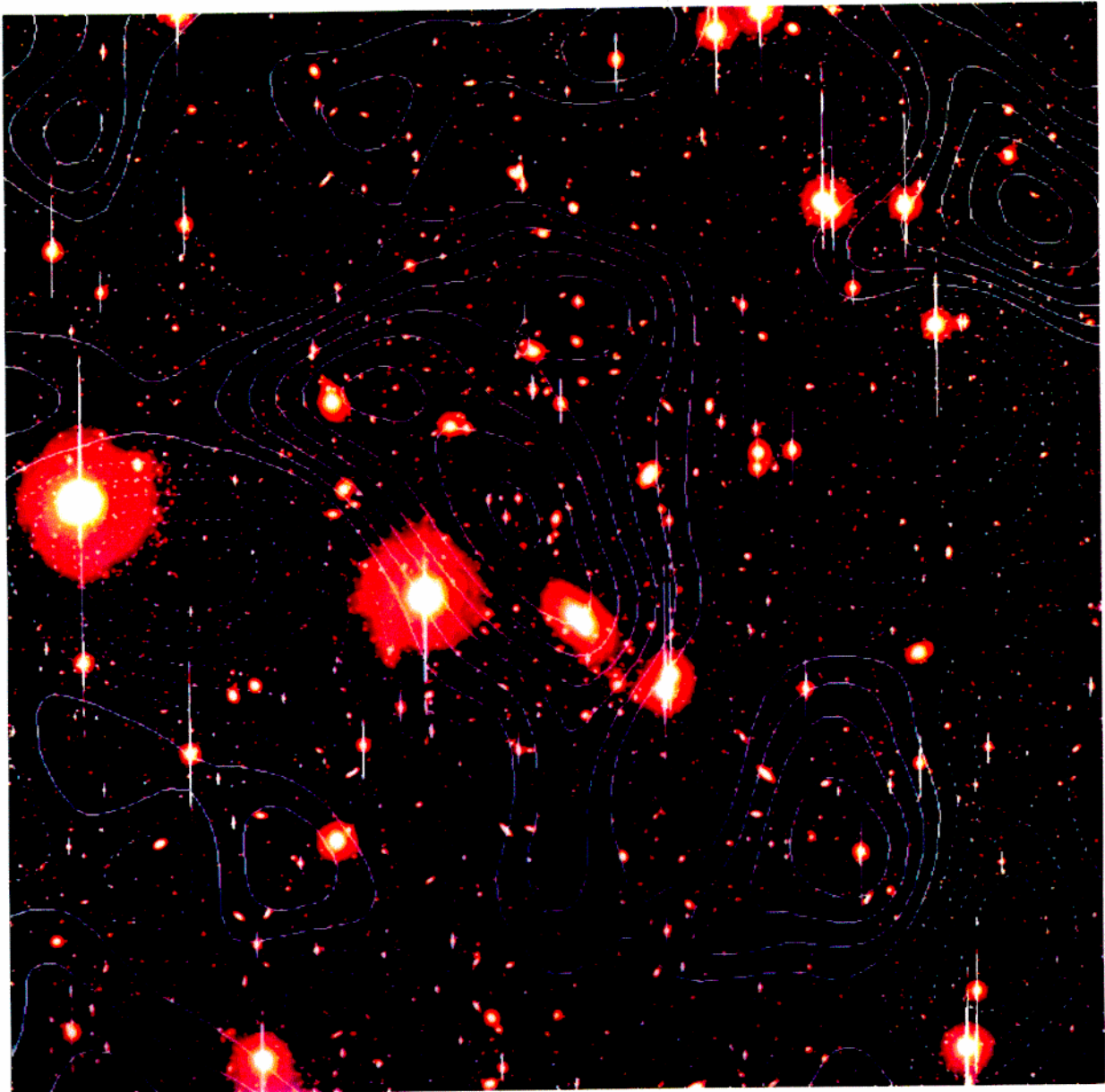
Hubble Plots



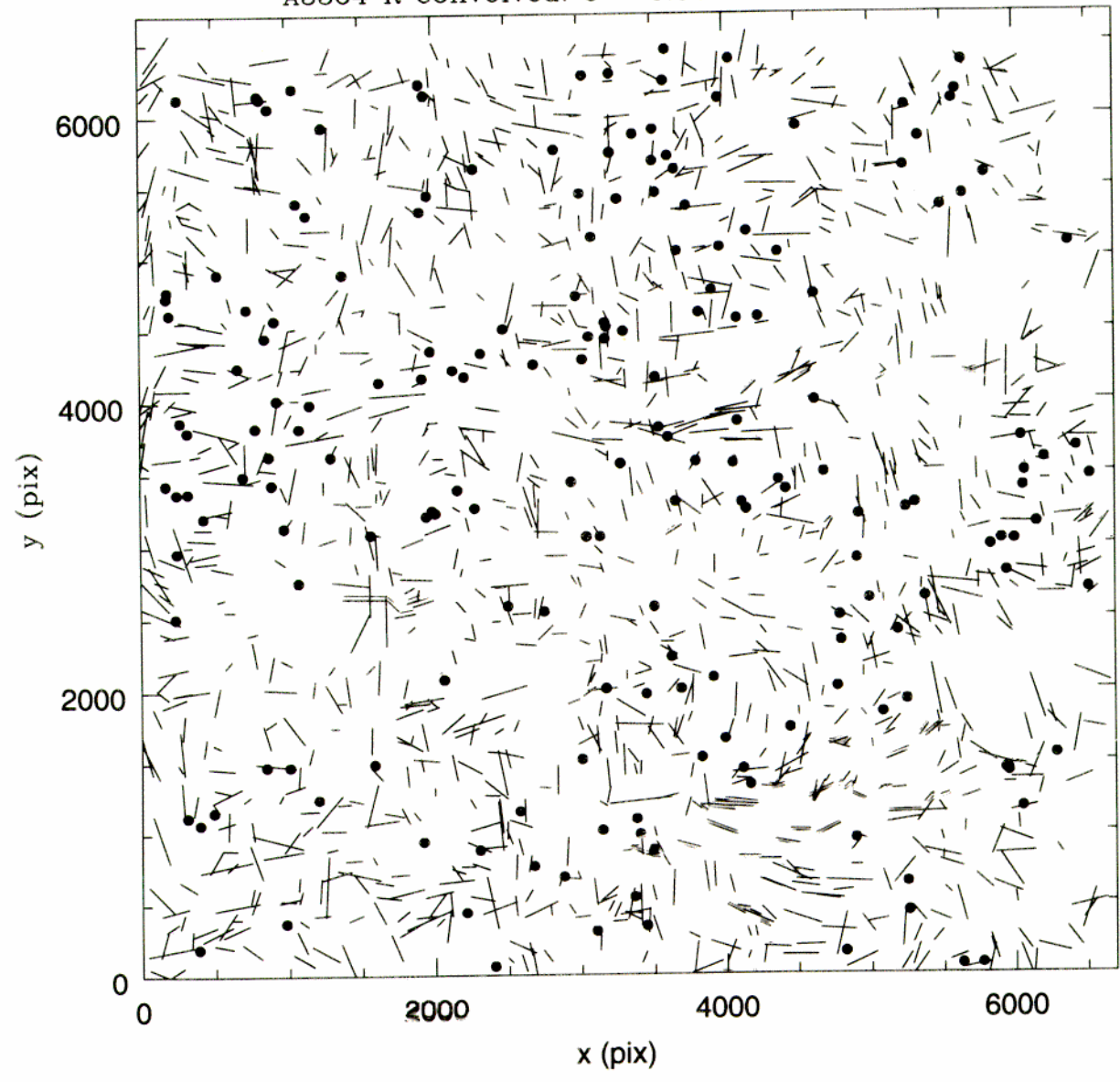


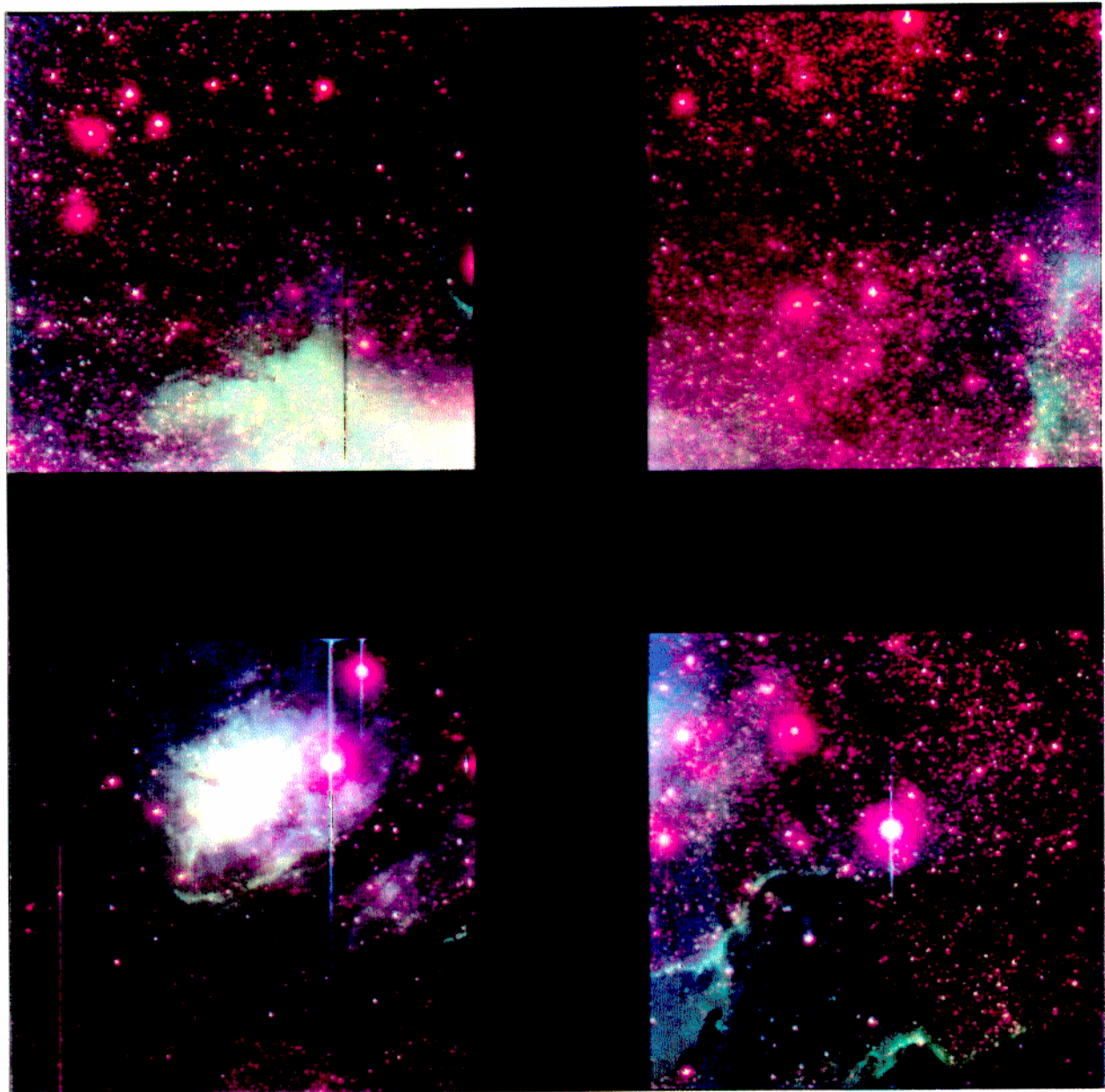
47ⁿ field
120,000 FBGs





A3364 R convolved: $e = 0.00076$





TkCCD Camera Interface

File **Setup** **Clear Chips** **Expert** **Special** **Help**

Current Exposure:

Basename:

Sequence Number:

Path:

Exposure Time:

Type: Bias

Buffer: 1 Filter: **Ictio**

Title:

Comment:

Abort

CCD Format: (Click chip to edit)

Name: <NoName>

1

2

4


3

Off 1x1 2x2 4x4 8x8 Other

Camera Status:

CCD Status: **READOUT**

Filter (Click to change) **Ictio**

Shutter Position: 

CCD Temps: 168.0 163.0 168.0 162.0

Readout Progress

640

0 (rows) 2048

Buffer Status:

Buffer No.: 1

600

0 Rows Written to Disk 2048

Path:

Name:

Status: ACTIVE Overwrite

Local Environment:

UT: 17:39:20.8 12/30/1997

Coords: 19:33:20.39 20:43:07.6 2000.0

Airmass:

File Host:

Observer:

Operator:

Next Exposure:

Basename:

Sequence Number:

Path:

Exposure Time:

Type: Bias Repeat:

Buffer: Any Filter: **Ictio**

Title:

Comment:

GO

CCD Format: (Click chip to edit)

Name: <NoName>

1

2

4

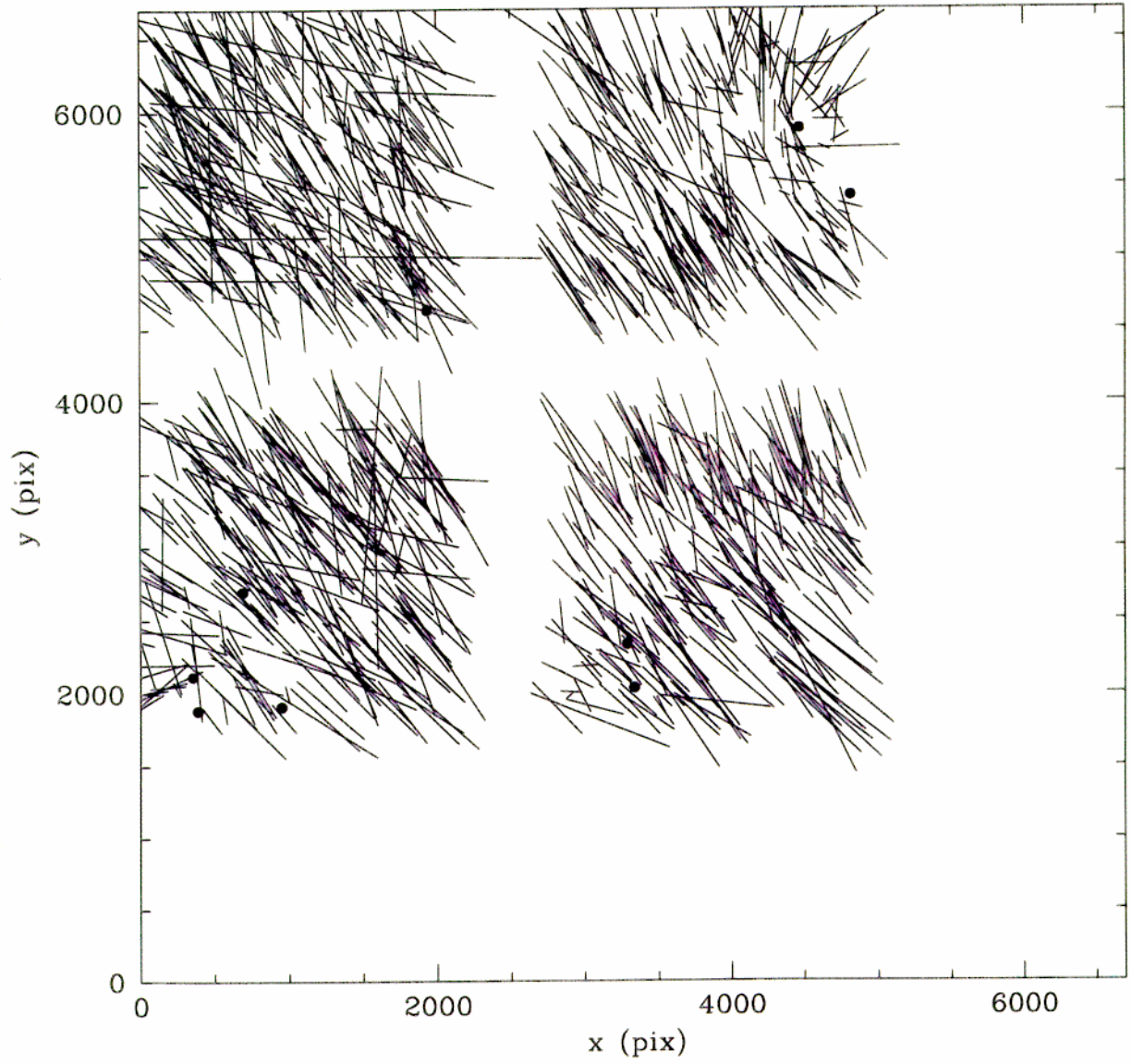
3

Off 1x1 2x2 4x4 8x8 Other

Elliptical stars

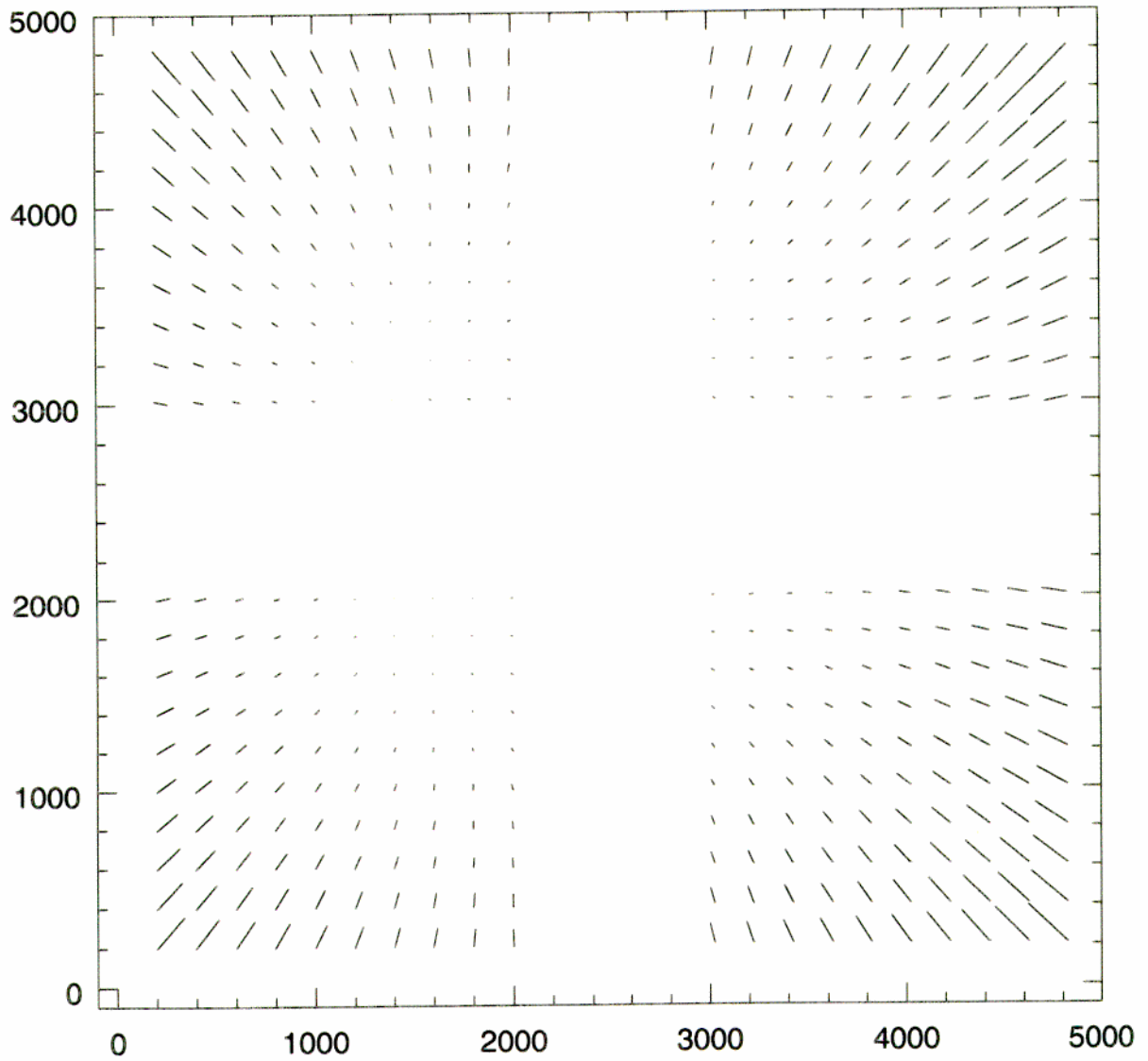
400 x

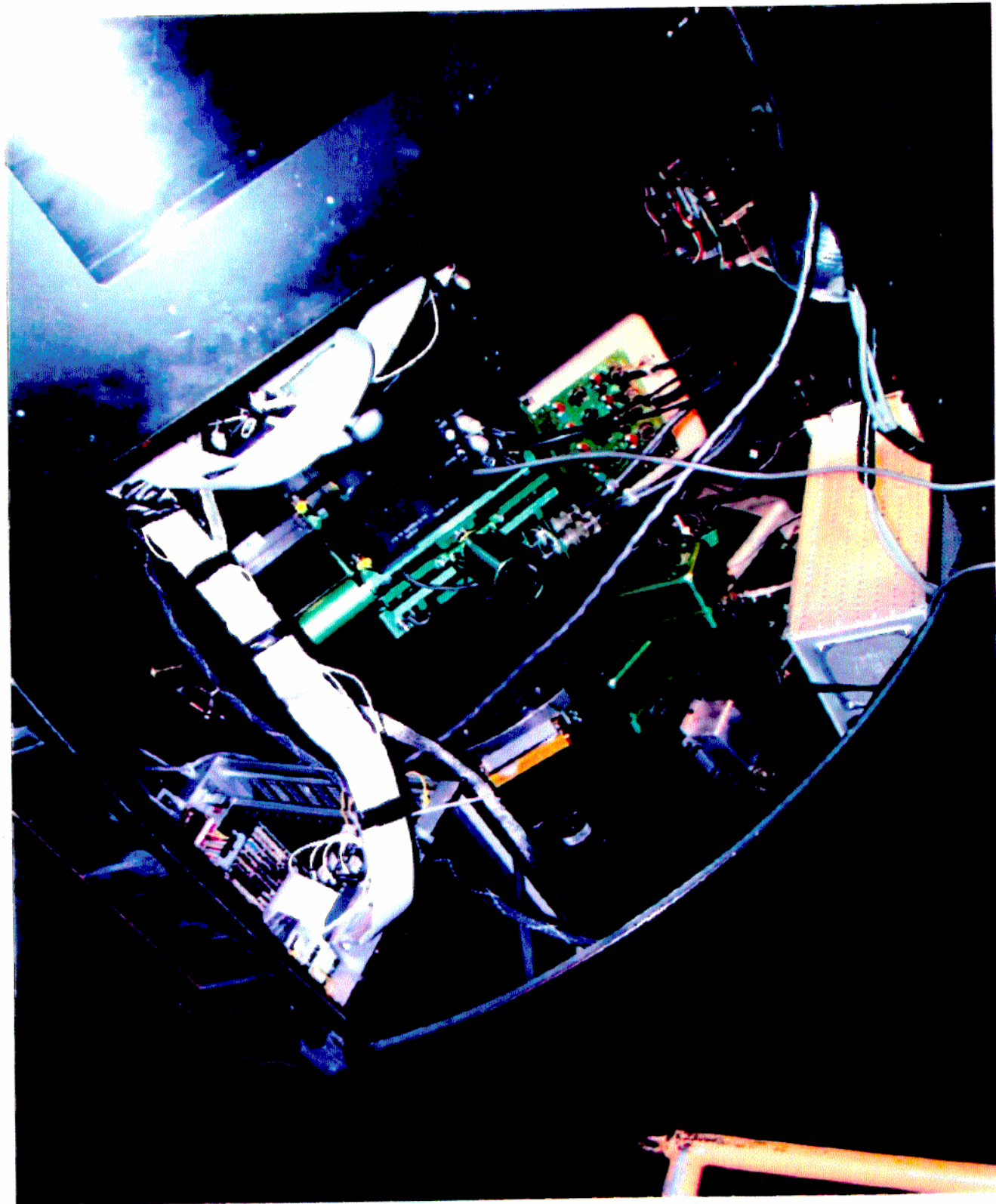
raw data: $e = 0.062$



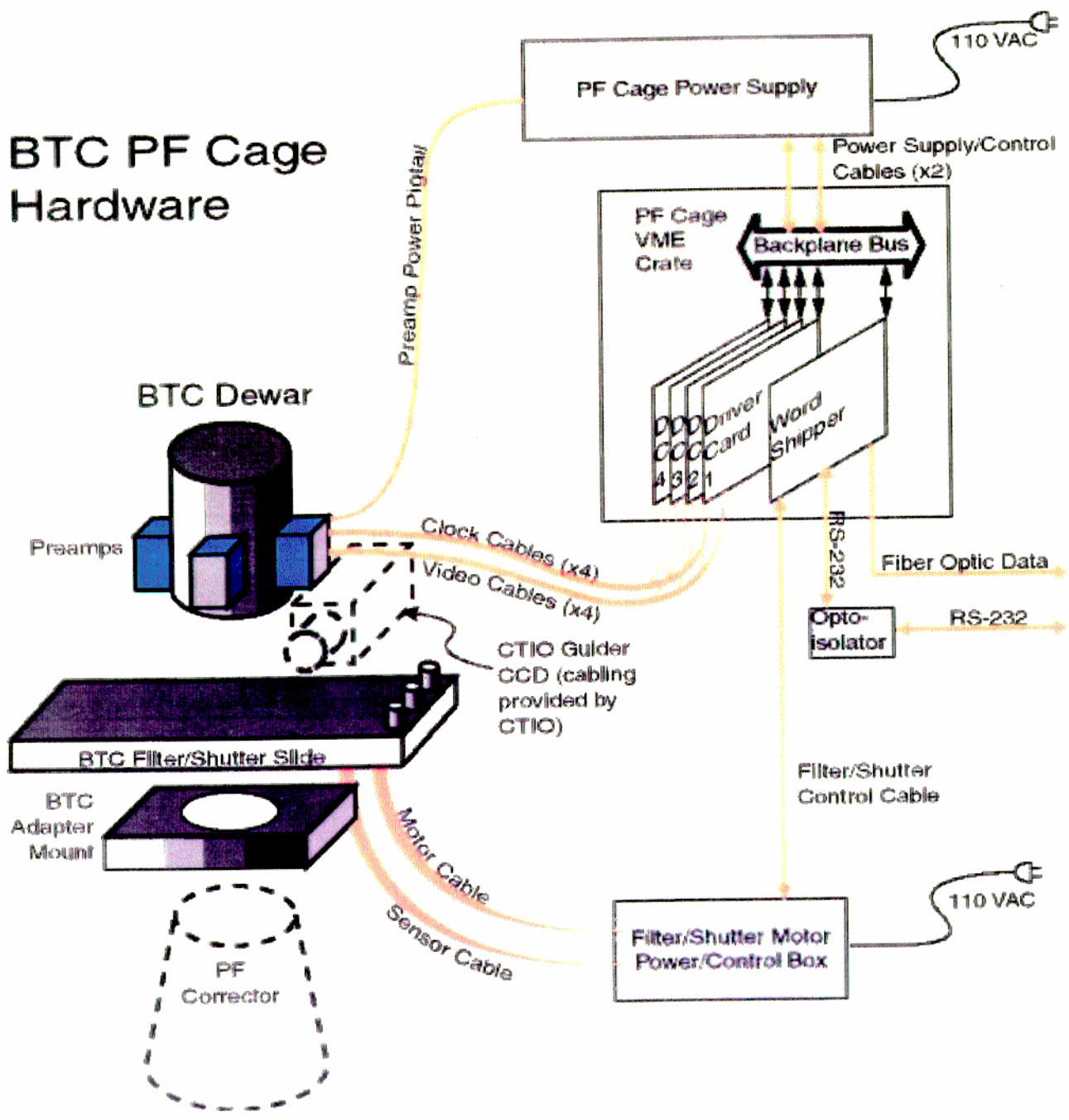
PF corrector field distortion

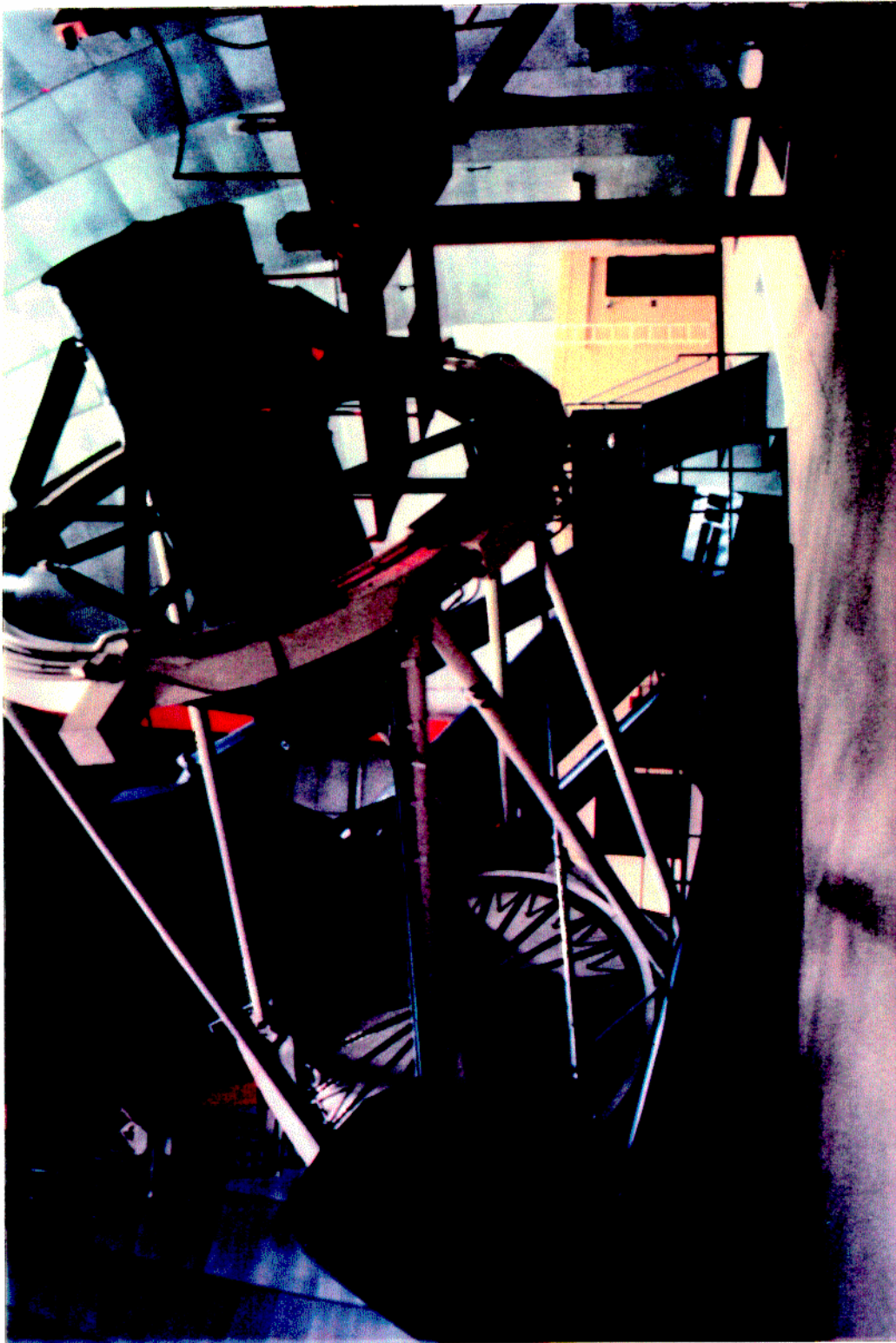
4x

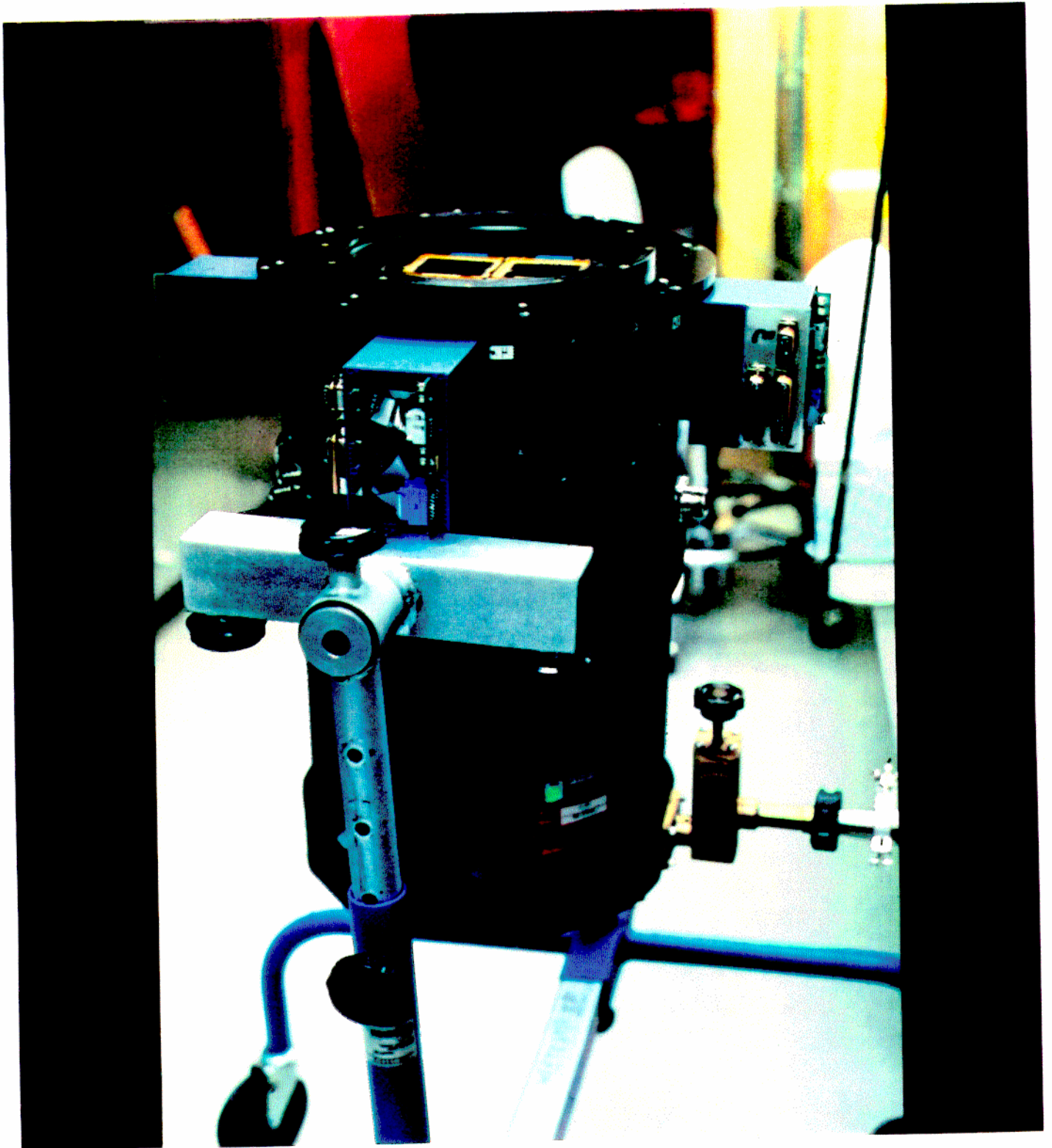


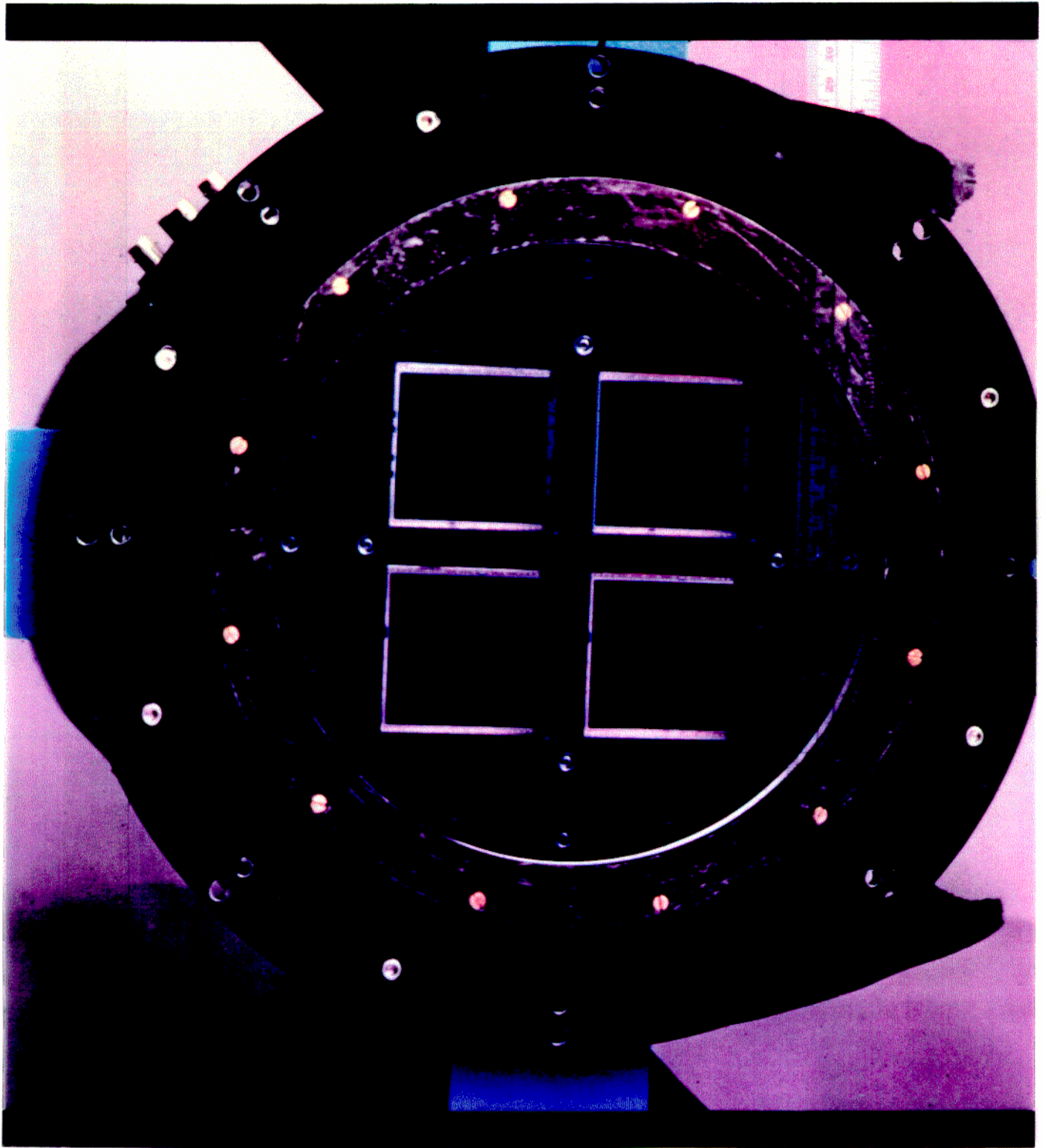


BTC PF Cage Hardware









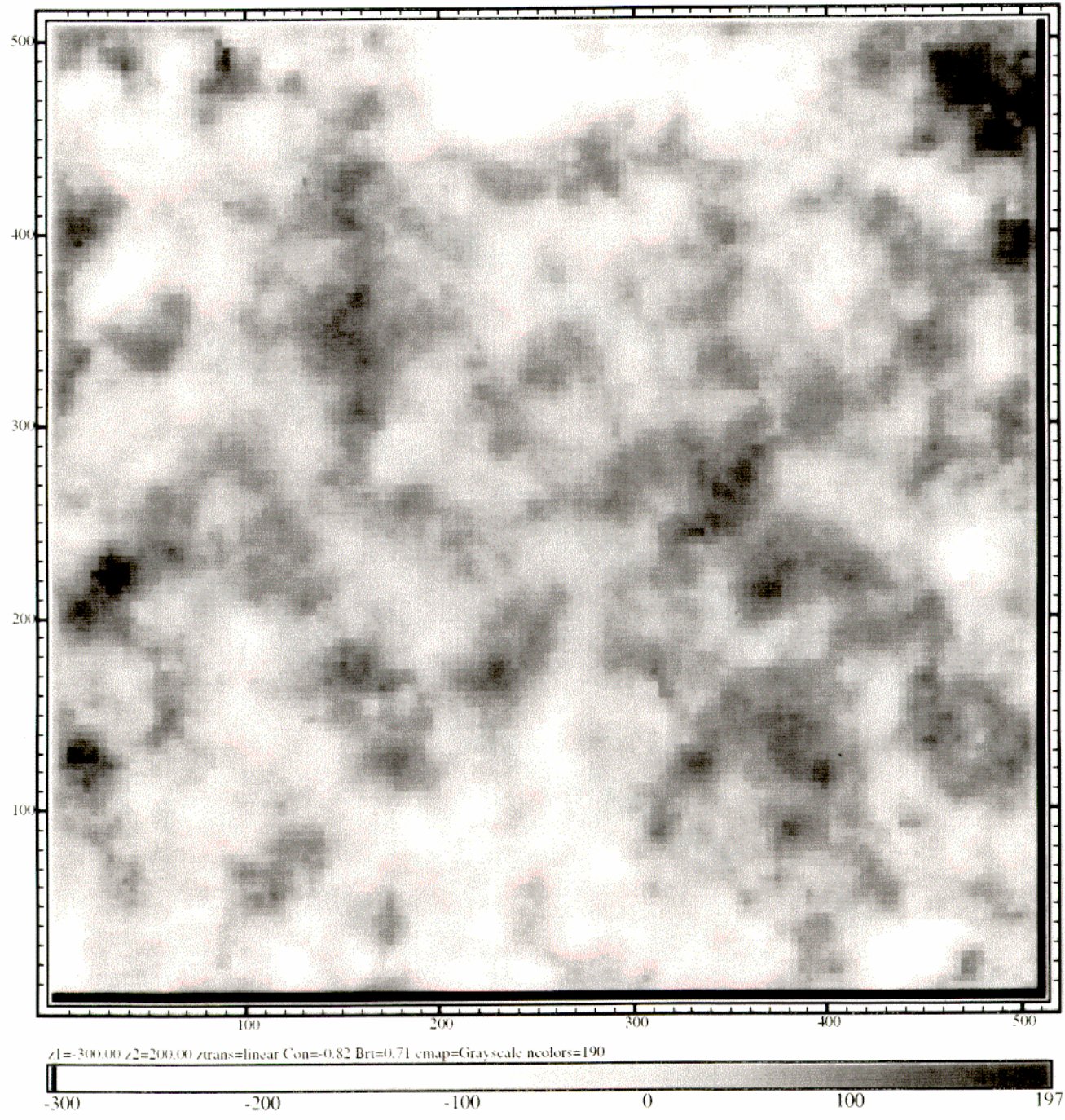
THE BIG THROUGHPUT CAMERA

I. Dell'Antonio, T. Tyson, D. Wittman (*Bell Labs*)

G. Bernstein, P. Fischer, G. Smith (*U. Michigan*)

R. Lee (*Lassen Research*)

- SEXTANS INVLENS



TVJM 84

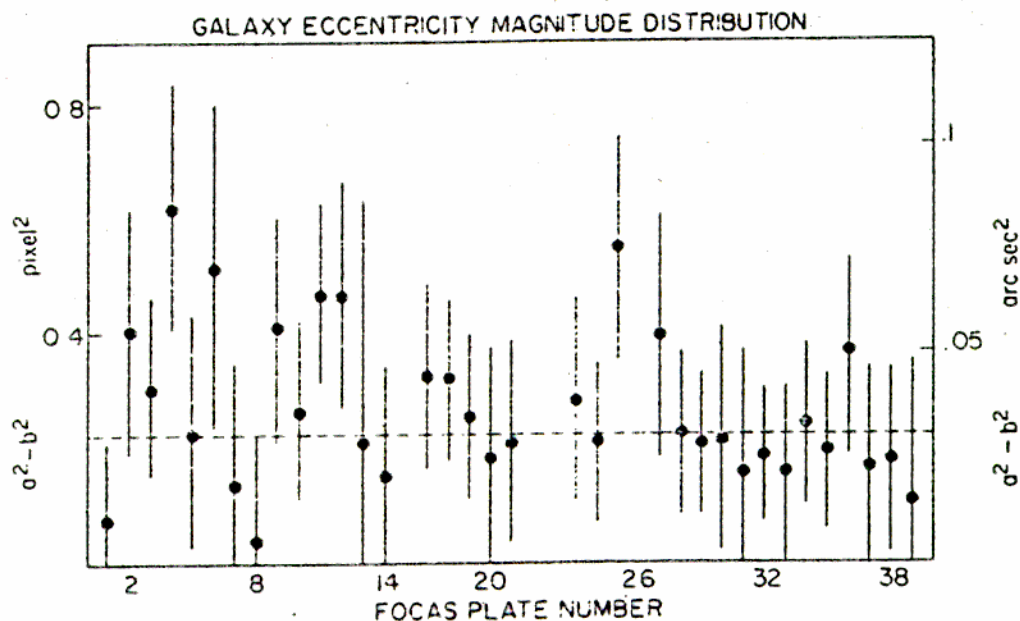


FIG. 1.—Magnitude $a^2 - b^2$ (from Table 4) of the galaxy eccentricity vector vs. increasing FOCAS plate number (see Table 1), for galaxies with $22.5 < J < 23.5$ mag. Error bars are 1σ . All plates have galaxy eccentricities consistent with zero within 2σ . Dashed line is expected (noise) and averaged eccentricity. The amplitude of the largest Weyl tensor component $c^2 CH_0^{-2}$ is very nearly given by $a^2 - b^2$ in units of square pixels.

$$\text{In-field} \quad \langle e - \bar{e} \rangle = 0.06$$

$$\text{Field-field} \quad \langle e - \bar{e} \rangle = 0.03$$

$$\text{Global} \quad \bar{e} = 0.01 \pm 0.01$$

OBSERVATIONS IN COSMOLOGY

J. KRISTIAN* AND R. K. SACHS

Relativity Center, The University of Texas, Austin, Texas

Received May 7, 1965

ABSTRACT

Observations of cosmological effects in anisotropic, inhomogeneous cosmological models are discussed in detail, with numerical estimates. The first and last sections of the paper form a self-contained unit for readers who are unfamiliar with Riemannian geometry. The other sections contain mathematical derivations.

Three assumptions are made: (i) that the universe is described by a Riemannian space time with slowly varying metric tensor; (ii) that light travels along null geodesics and obeys the usual area-intensity law; and (iii) that the gravitational field is related to the matter by Einstein's field equations for dust. The third assumption is not needed for many of the results; the second assumption is proved in the geometric optics limit, assuming a general relativistic model.

The importance of trying to observe angular variations in the various cosmological effects is emphasized. It is shown that otherwise unobservable anisotropies or inhomogeneities can easily give the observed order of magnitude and either sign for the acceleration parameter measured in any one direction via redshifts. A model-independent law for the apparent area of a distant object is given. Detailed equations for number counts and for apparent proper motions are given. It is pointed out that observations to date do not exclude the possible presence of anisotropies and inhomogeneities whose dynamical effects are comparable to the dynamical effects of the expansion.

A new effect, the "distortion effect," is discussed. In any anisotropic model, all distant objects in a particular direction on the celestial sphere may appear distorted, with a definite preferential direction for their longest dimension. The effect gives a direct measurement of space-time curvature and may be observable. But a positive result of the measurement would not favor general relativity over other theories in which assumptions (i) and (ii) above hold.

I. INTRODUCTION

In cosmology, the universe is usually assumed spatially isotropic or at least homogeneous, except for local irregularities whose distance scale is too small to have cosmological significance (Heckmann and Schücking 1959, 1962; McVittie 1956, 1959, 1962; for inhomogeneous models see Bondi 1947; Hoyle and Narlikar 1961). The observational basis of this assumption is dubious, however, in view of the scarcity of observations near the galactic plane and recent evidence pointing to possible superclustering of galaxies. Therefore, it seems reasonable to ask what observational consequences anisotropies or large-scale inhomogeneities would have. In this paper we attempt to answer this question systematically. We are mainly interested in inhomogeneities whose scale is something like 10^9 light-years or more, with smaller scale variations smoothed out as before, though we shall also briefly discuss the possibility that fluctuations whose scale is several orders of magnitude smaller might have measurable effects which would give information on the curvature of space-time. A detailed presentation of our results, with all technical details suppressed and with a Newtonian notation, is given in § III.2.

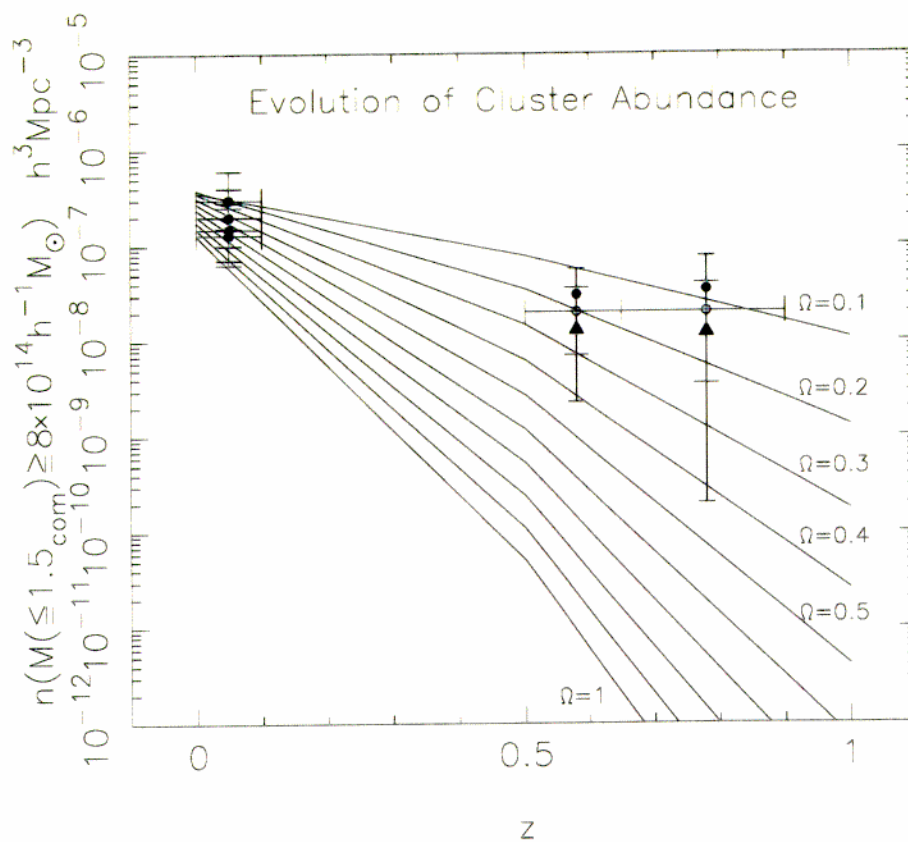
Inhomogeneities and anisotropies have not been much discussed in the literature because finding a global cosmological model which does not have a high degree of symmetry is very difficult. But a global model, with boundary conditions and everything else included, is far more than we need to discuss most of the observations that might be made in the near future (see, e.g., Sandage 1961). If we concentrate on those features of any model that have the most direct observational significance, then a very general treatment can be given using standard mathematical techniques.

We make three fundamental assumptions in this paper. In order of importance, these

* Present address: Washburn Observatory, University of Wisconsin, Madison, Wisconsin.

Two too many high- z clusters

N. Bahcall & X. Fan, PNAS, 1998, 95



but: non-Gaussian fluctuations?

Figure 2. Evolution of the number density of massive clusters as a function of redshift: observed versus expected (for clusters with mass $\geq 8 \times 10^{14} h^{-1} M_{\odot}$ within a comoving radius of $1.5 h^{-1} \text{Mpc}$). From Bahcall and Fan 1998 (29). The expected evolution is presented for different Ω_m values by the different curves. The observational data points (see text) show only a slow evolution in the cluster abundance, consistent with $\Omega_m \simeq 0.2_{-0.1}^{+0.15}$. Models with $\Omega_m = 1$ predict $\sim 10^5$ fewer clusters than observed at $z \sim 0.8$, and $\sim 10^3$ fewer clusters than observed at $z \sim 0.6$.

Summary

Lensing vs X-ray

Overall $M_L \sim 2M_x$

BUT:

Discrepancy only in cluster cores

Mass model problem?

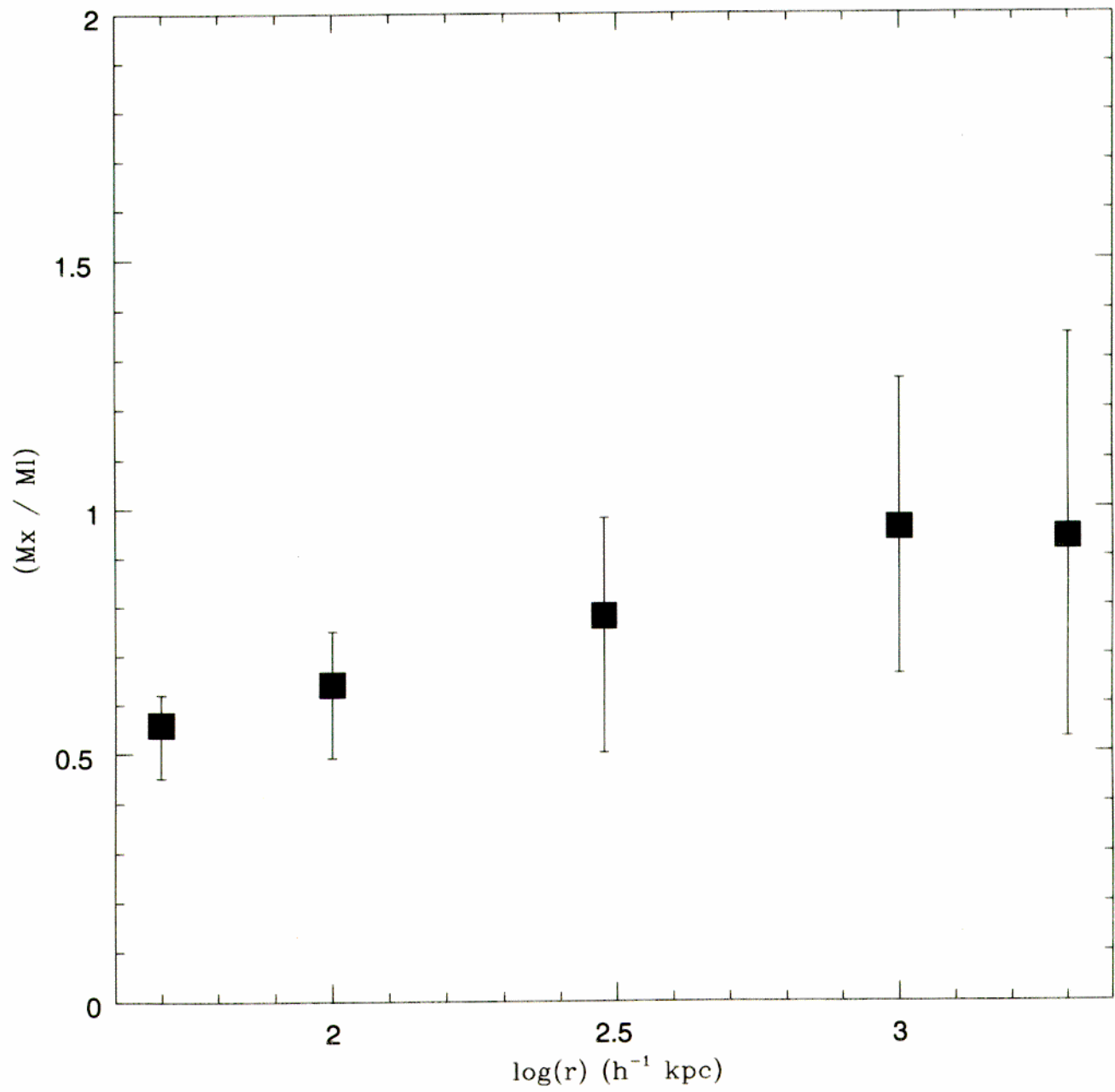
Cooling Flows important

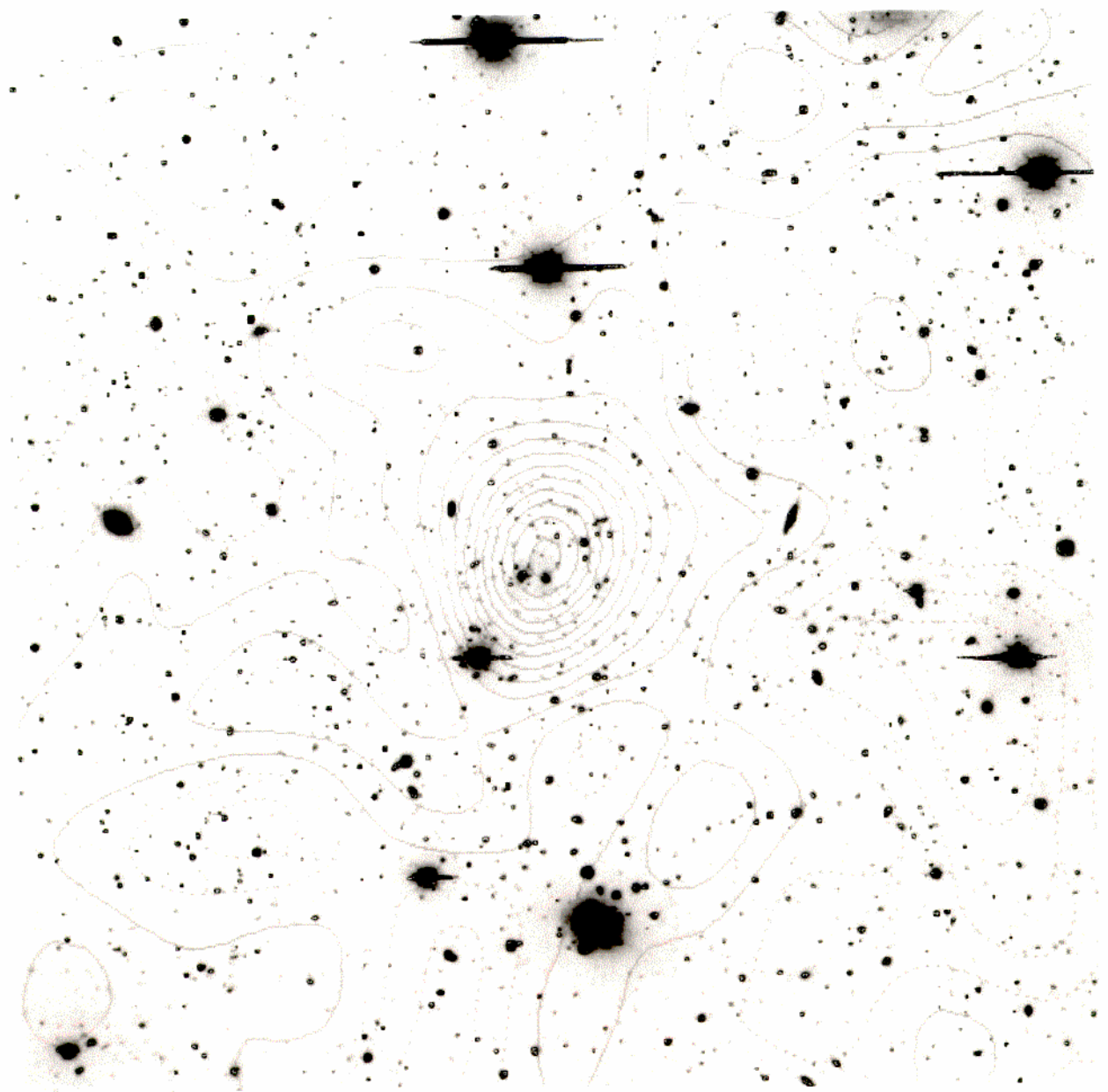
Accurate lens modeling helps

Remaining Discrepancies tell
about state of cluster core

This is Useful! example:

M_x/M_L vs z Tests Structure Formation



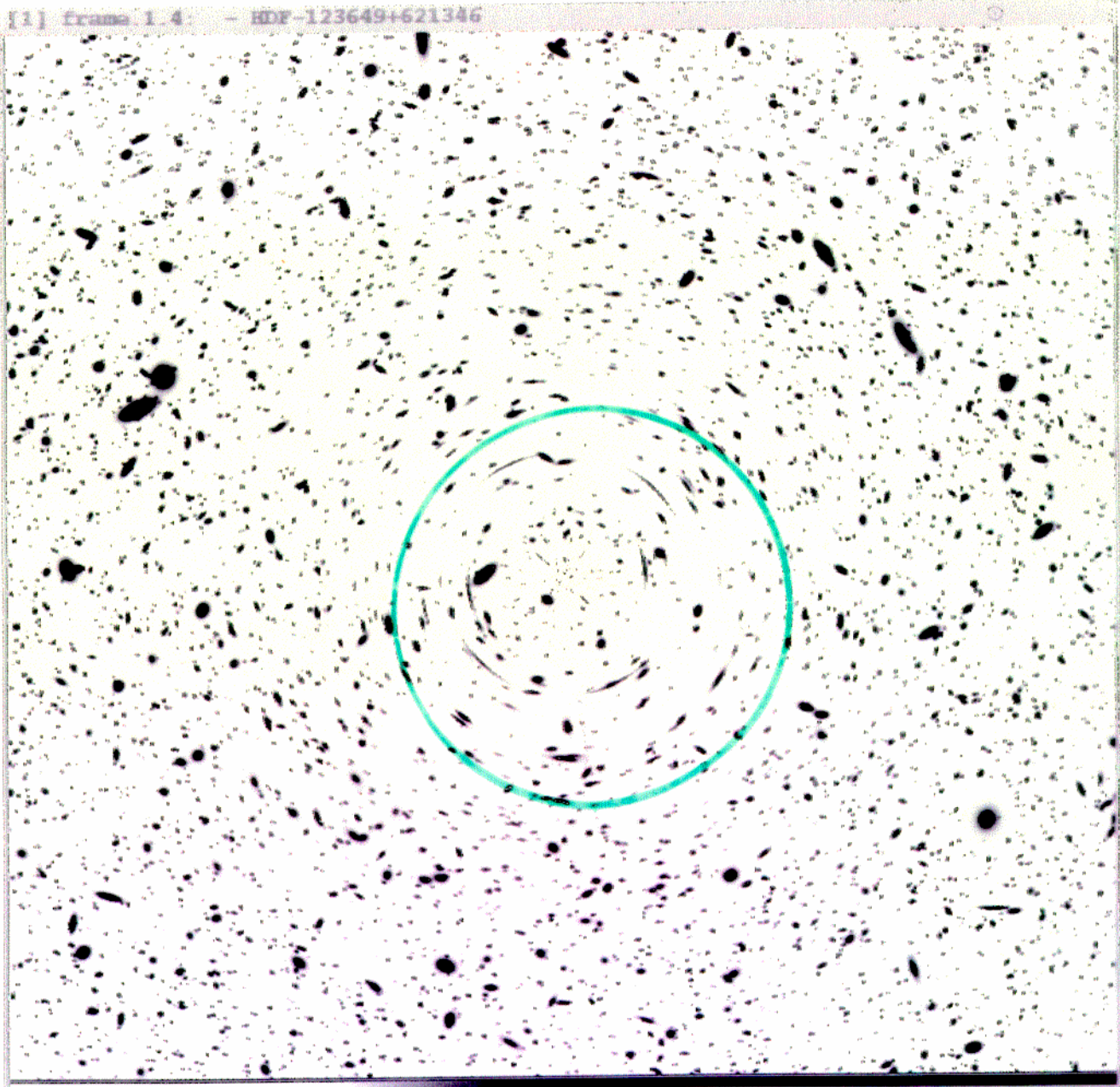


INVERTING THE ARCLETS

$$D(r) = \frac{a^2 - b^2}{a^2 + b^2}$$

$$\bar{\Sigma}(r) = \frac{2\Sigma_c C}{(1 - r^2/r_{max}^2)} \int_r^{r_{max}} dr \frac{D(r)}{r} + \bar{\Sigma}(r, r_{max})$$

[1] frame 1.4: - HDF-123649+621346



Circular potential

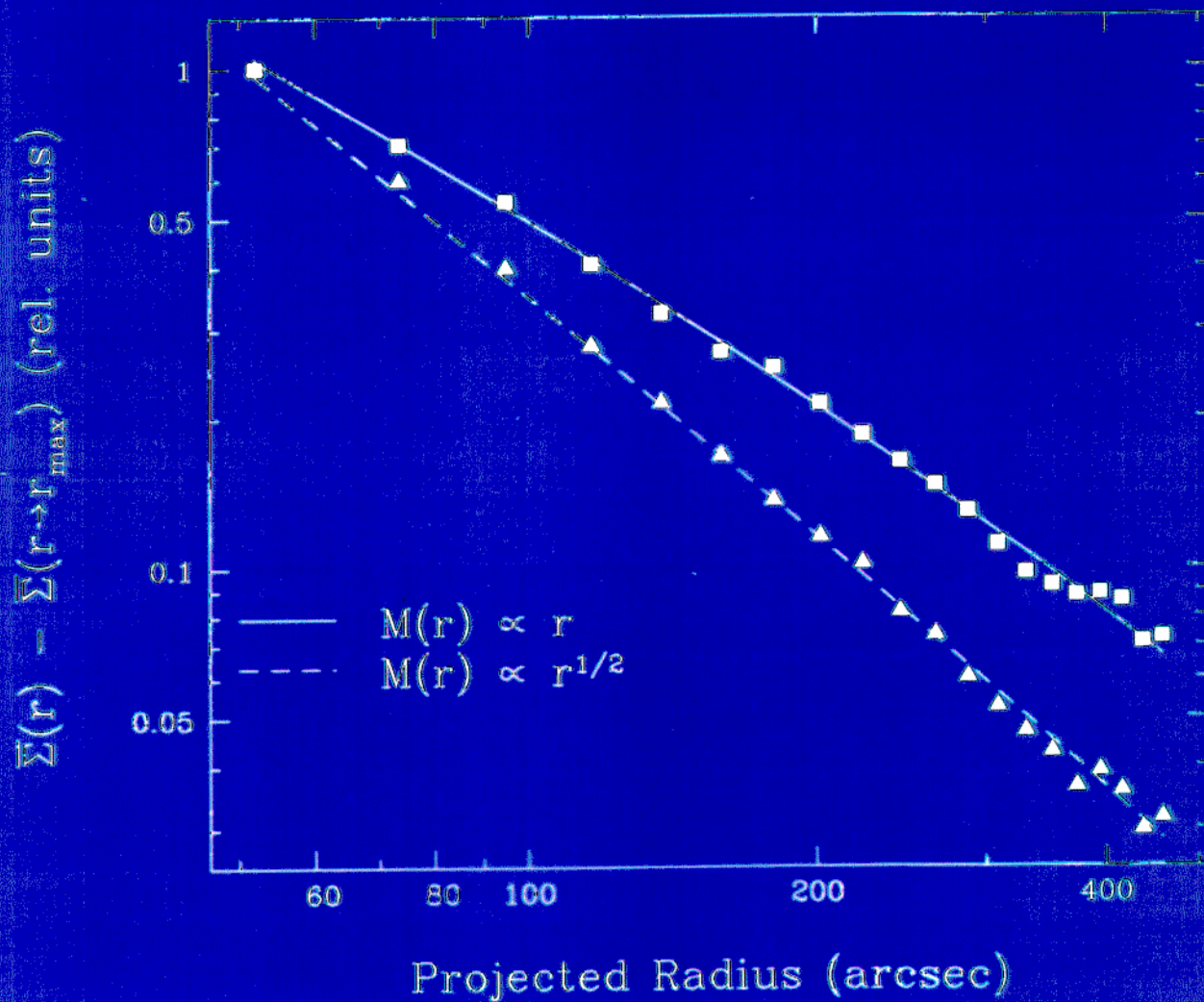
$$\text{Shear } \gamma(r) = \frac{\bar{\Sigma}(\langle r \rangle)}{\Sigma_c} - \frac{\bar{\Sigma}(r)}{\Sigma_c}$$

$$\int_{r_1}^{r_2} \frac{\gamma(r)}{r} dr = \frac{1}{2} \Sigma_c^{-1} \left[\bar{\Sigma}(\langle r_1 \rangle) - \bar{\Sigma}(\langle r_2 \rangle) \right]$$

$$\bar{\Sigma}(\langle r_1 \rangle) - \bar{\Sigma}(\langle r_2 \rangle) = 2 \Sigma_c \int_{r_1}^{r_2} \frac{\gamma(r)}{r} dr$$

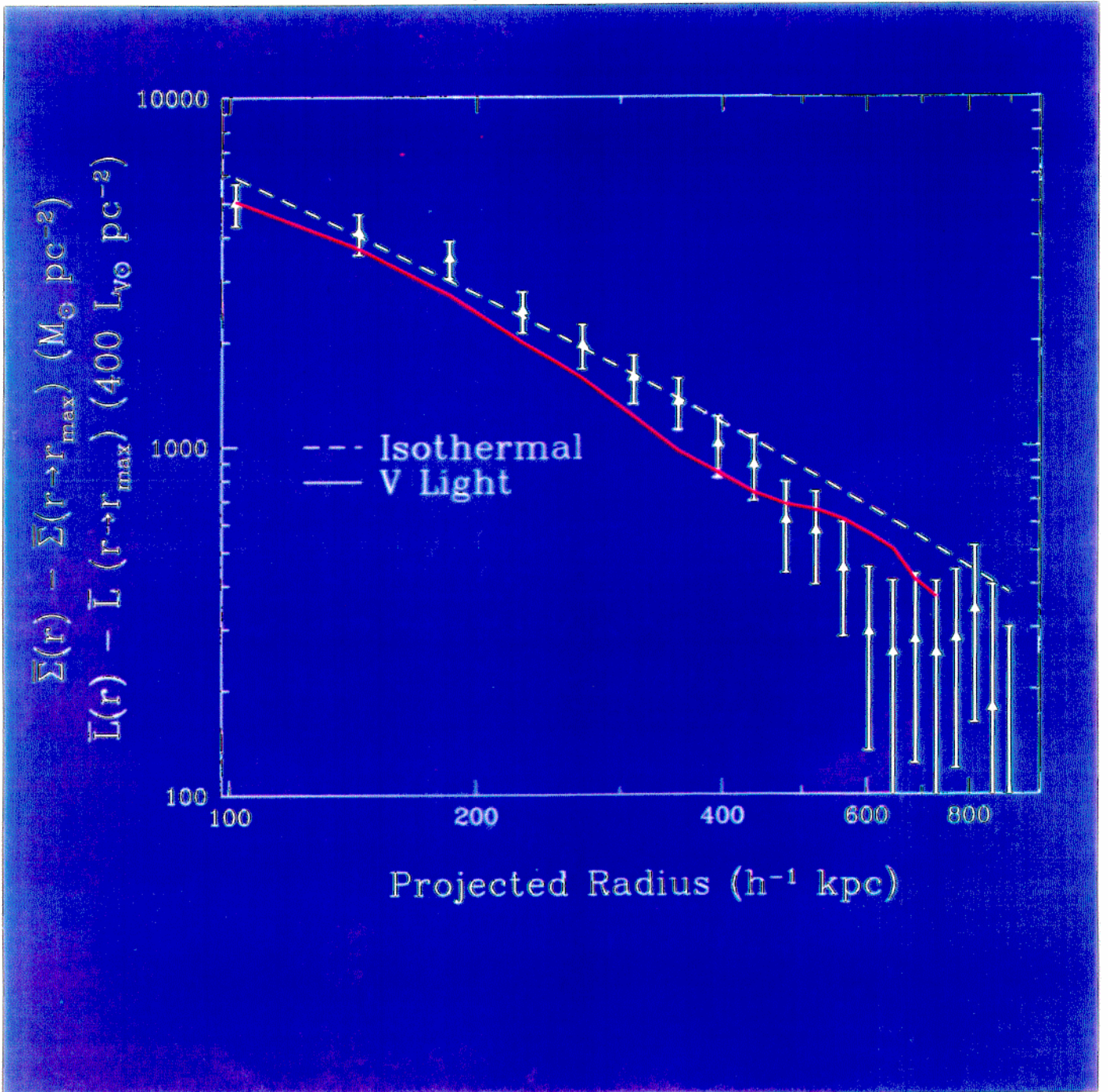
$$\Sigma_c = \frac{c^2}{4\pi G} \frac{D_s}{D_L D_{Ls}} \quad \text{g cm}^{-2}$$

Simulated data + inversion

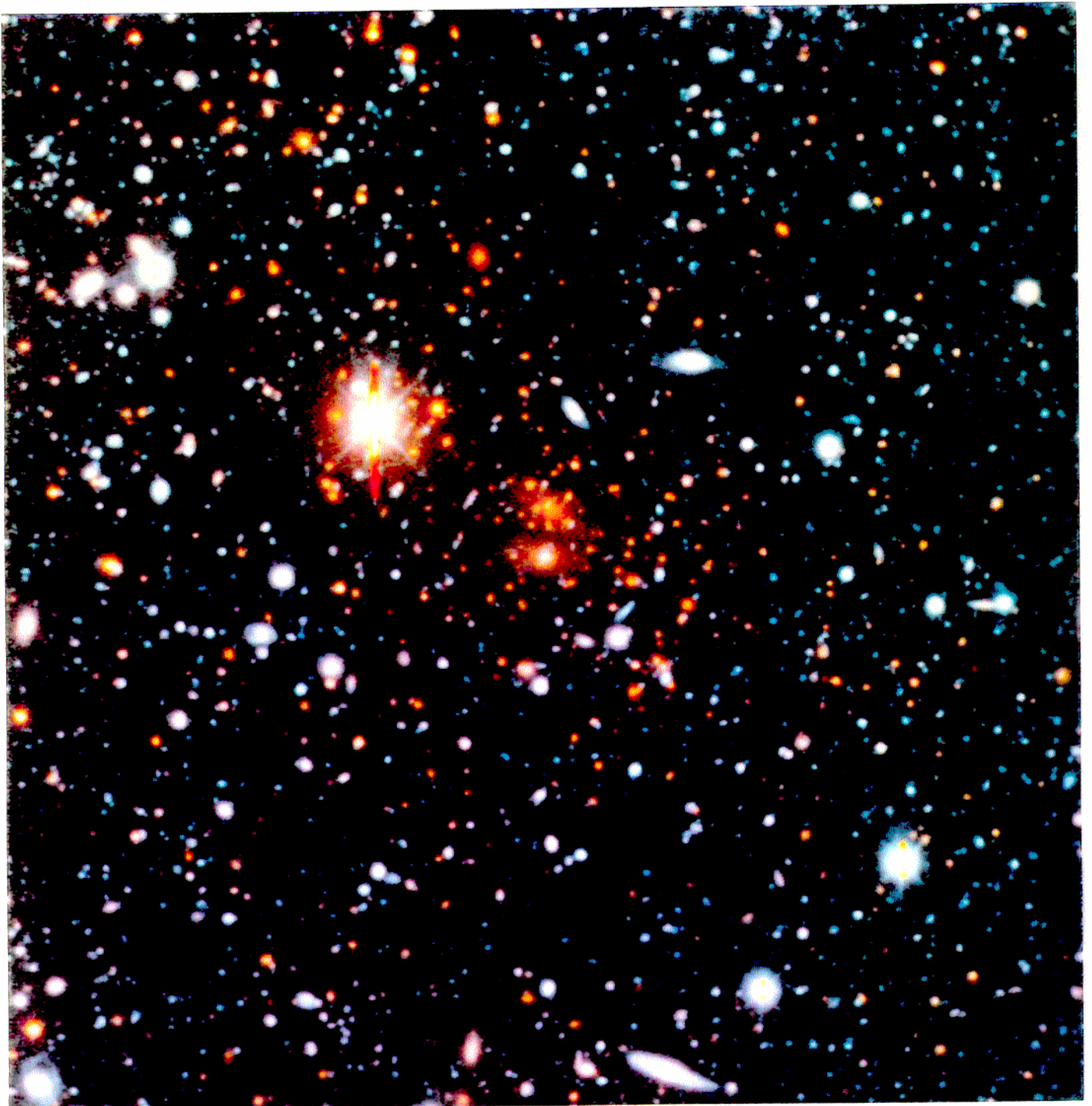


Tyson + Fischer 1995

A 1689



RXJ 1347-1145

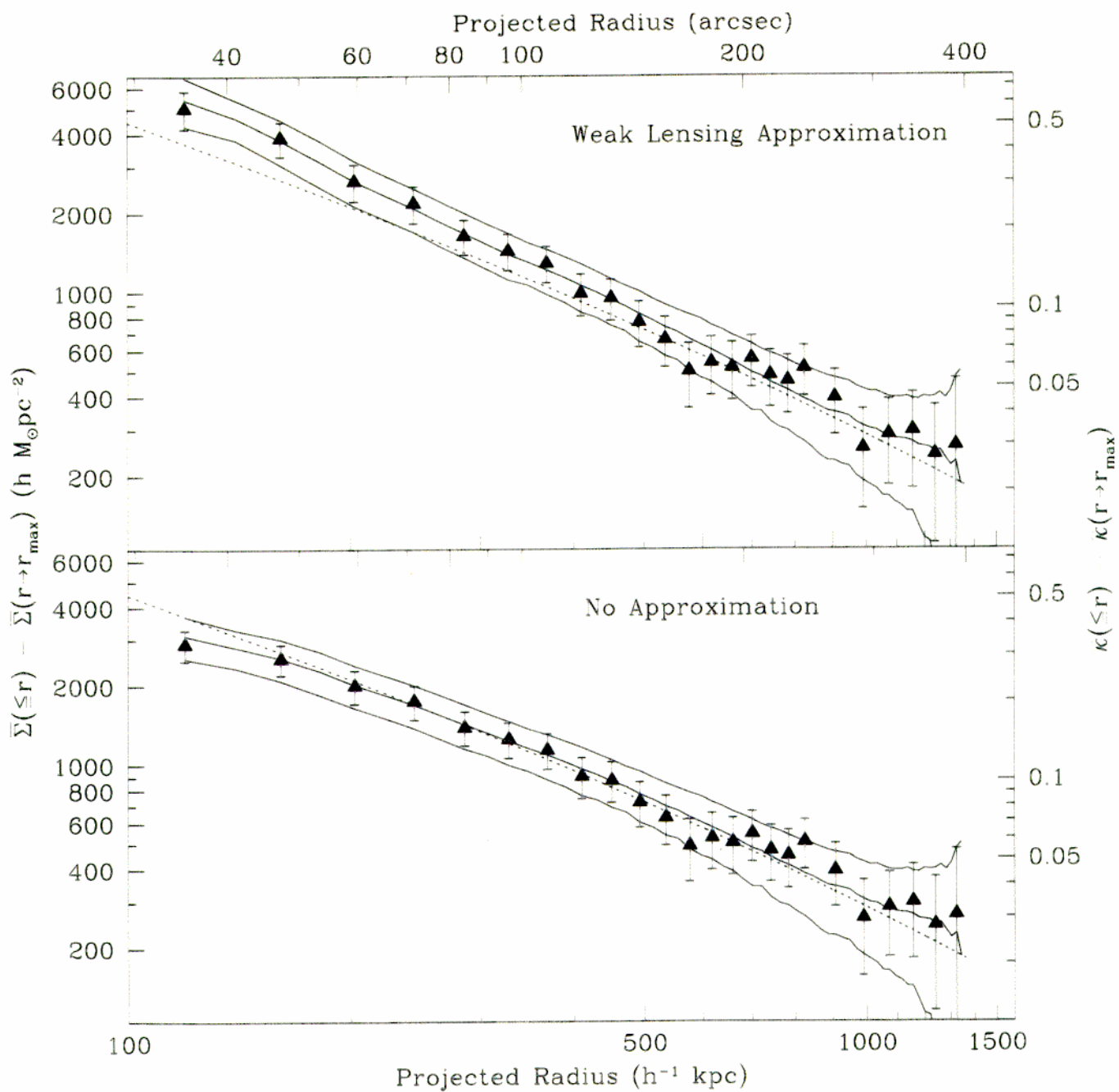


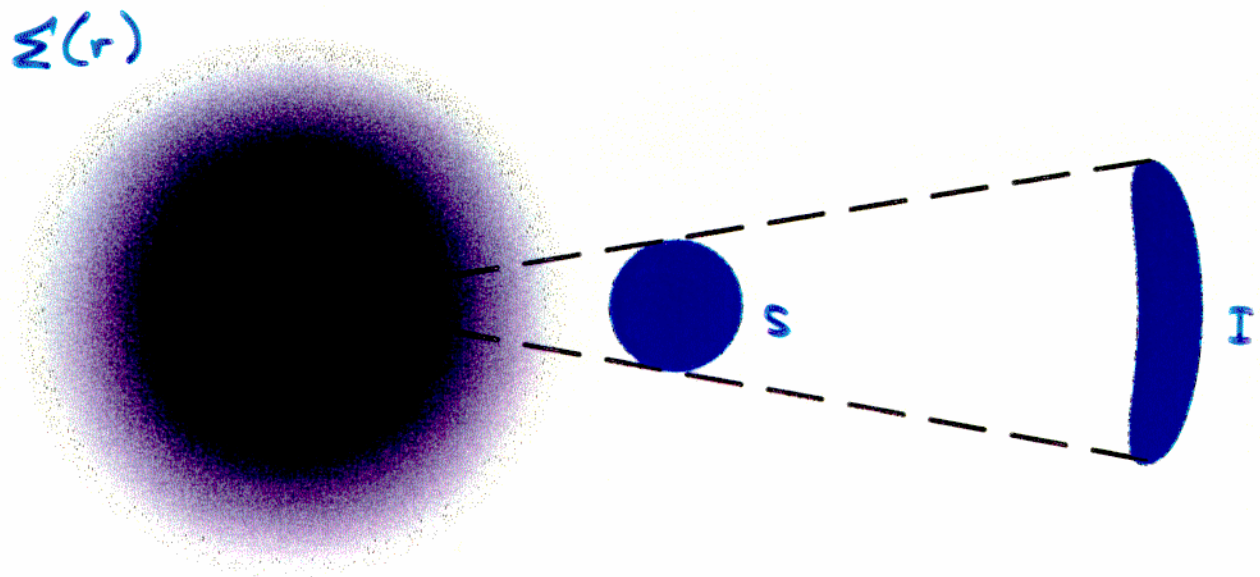
$$\kappa(r) = \Sigma(r) / \Sigma_c \quad \text{convergence}$$

$$\gamma(r) = \Sigma_c^{-1} (\bar{\Sigma}(r) - \Sigma(r)) \quad \text{shear}$$

$$T(r) = \frac{i_{\theta\theta} - i_{rr}}{i_{\theta\theta} + i_{rr}} = \frac{2 \gamma_t(r) [1 - \kappa(r)]}{[1 - \kappa(r)]^2 + \gamma_t^2(r)}$$

Fischer + Tyson 1996



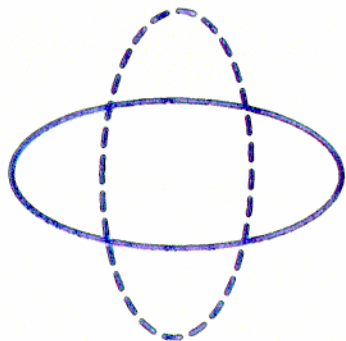


$$x, y \rightarrow r, \theta$$

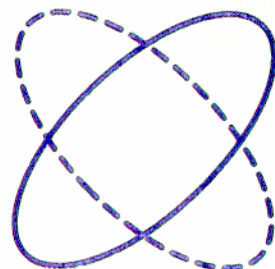
$$\text{Shear } \gamma = \langle \varepsilon_{\theta} \rangle$$

$$\gamma = [\bar{\Sigma}(\langle r \rangle) - \Sigma(r)] / \Sigma_{\text{crit}}$$

$$\bar{\Sigma}(\langle r_1 \rangle) - \bar{\Sigma}(\langle r_2 \rangle) = \Sigma_c \int_{r_1}^{r_2} \gamma(r) K(r) dr$$



$$I_{xx} - I_{yy}$$



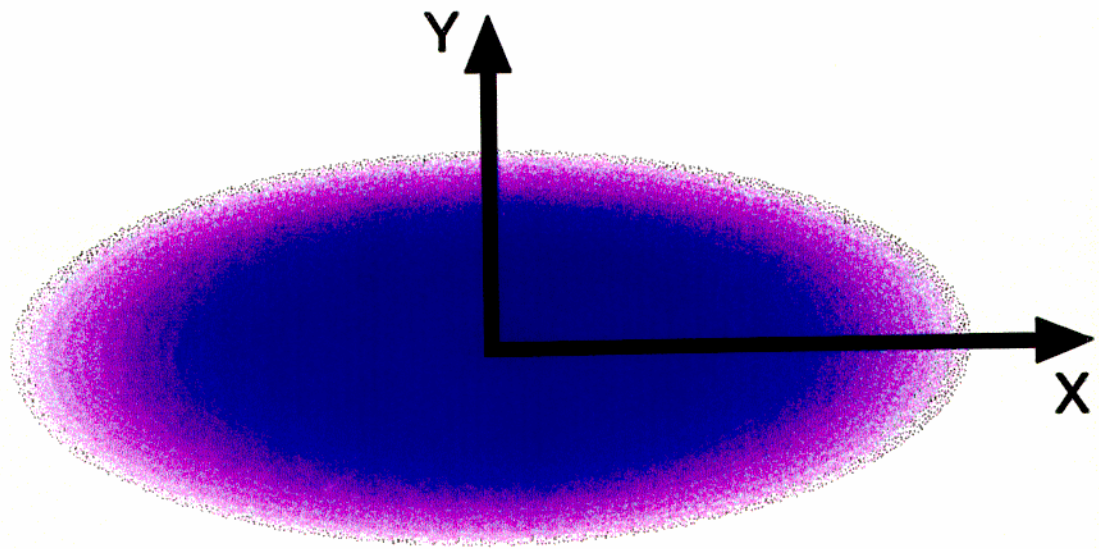
$$2I_{xy}$$

$$\epsilon_1 = \frac{I_{xx} - I_{yy}}{I_{xx} + I_{yy}}$$

$$\epsilon_2 = \frac{2I_{xy}}{I_{xx} + I_{yy}}$$

$$\epsilon_1 = \epsilon \cos 2\eta$$

$$\epsilon_2 = \epsilon \sin 2\eta$$



$$I_{xx} = \int I(x,y) x^2 dx dy$$

$$I_{xy} = \int I(x,y) xy dx dy$$

$$I_{yy} = \int I(x,y) y^2 dx dy$$

EXPLORING DARK MATTER WITH GRAVITATIONAL LENS TOMOGRAPHY

Inverse Problem: Solve for foreground mass overdensity which produces the statistical distortions in distant galaxy images

- Quantitative measure of the distribution of dark matter in the universe
- This “weak” lensing inversion may be applied to overdensities on scales from 10 kpc to 10 Mpc
- The high density of background faint blue galaxies are ideal sources